J. Min. Metall. Sect. B-Metall. 51 (2) B (2015) 179 - 184

Journal of Mining and Metallurgy, Section B: Metallurgy

INTERFACIAL REACTIONS BETWEEN SOLID Ni AND LIQUID Sn–Zn ALLOYS

V. Gandova

University of Food Technologies, Inorganic and Physical Chemistry Department, Plovdiv, Bulgaria

(Received 01 November 2014; accepted 01 September 2015)

Abstract

The limitation of the harmful lead-containing solders used in the electronics and other industry applications change lead with another metals. Interfacial reactions between Sn–Zn alloys and Ni substrate after annealing at 400 and 450°C were studied. Three intermetallic compounds Ni_3Sn_4, T1, γ-Ni_5Zn_{21} and liquid Sn were observed in the Ni/Sn–Zn diffusion couples. Scanning electron microscope was used for the investigation of the microstructure. The microhardness measurement of the intermetallic layers was also performed.

Keywords: solders, ternary systems, diffusion couples, phase diagrams

1. Introduction

In the electronic industry the joining of various modules is essential process relying largely on the use of soldering technologies. The usage of Pb-containing solders has been restricted due to the lead toxicity [1], which resulted in a development of new lead-free solder materials. Prospective lead-free solders on the basis of tin-dominated alloys with small additions of silver and copper were developed [2]. Another promising candidates are the Sn–Zn alloys although they possess some weaknesses [3]. Similarly to the Sn–Pb binary system, the Sn–Zn has a simple binary phase diagram with a single eutectic without intermetallic compounds. Ni substrate is among the components of future solder alloys as it is often used for metallization in electronic devices.

The purpose of the present work is to study the intermetallic compounds in the binary systems within the ternary Ni–Sn–Zn and to confirm the existence of ternary phases known from previous investigations.

2. Literature review of previous investigations of the systems

2.1. Ni–Sn system

Ni–Sn system is a relatively complex one. The high-temperature phase Ni_3Sn_2_HT occurs between 483°C and 1267°C. The low-temperature phase of Ni_3Sn_2_LT is stable below 575°C. The Ni_3Sn_4 phase, which has a small homogeneity region, exists below 796°C.

Ghosh [4] and Miettinen [5] derived thermodynamic parameters for the Ni–Sn binary system. Ghosh adopted the Bragg-Williams-Gorsky model to treat the order-disorder transition of the Ni_3Sn_2 compound. However, when an extended multi-component system comprises the Ni–Sn binary system this model might not be suitable due to the second order transition in the Ni_3Sn_2 region.

Liu et al. [6] treated the Ni_3Sn_2 transition as a first-order transition. In the Ni–Sn binary system, five intermetallic compounds are formed: Ni_3Sn_HT, Ni_3Sn_LT, Ni_3Sn_2_HT, Ni_3Sn_2_LT, and Ni_3Sn_4. The formation enthalpies of Ni–Sn intermetallic compounds were obtained by Vassilev et al. [7] and by Flandorfer et al. [8] and the results are in a good agreement.

Riesenkampf et al. [9] found new (metastable) phase with composition close to $NiSn_9$ in Ni–Sn electrodeposits with 3-34 at.% Ni. At 100°C this phase decomposes to β-Sn and Ni_3Sn_4. Recently, Glibin et al. [10] suggested new thermodynamic assessment of nickel-tin solid and liquid alloys using graphical and analytical methods.

2.2. Ni–Zn system

The Ni–Zn phase diagram is retained from the studies of Vassilev et al. [11, 12] and Xiong et al. [13]. Four intermediate compounds are found in this system: β, β1, γ, and δ phases. The β phase is a high-temperature phase (stable between 675°C and 1040°C); the β_1 phase is a low-temperature one while γ phase is a γ-brass type with a homogeneity range of 74-85 at.% Zn. The δ phase is formed at 88.9 at.% Zn and 489°C through a peritectic reaction and has a very narrow homogeneity range.

* *Corresponding author: gandova_71@abv.bg*

DOI:10.2298/JMMB141101021G

2.3. Sn–Zn system

The Sn–Zn binary system is a simple eutectic one with no intermetallic compounds. It was optimized by a number of authors starting with Srivastava and Sharma [14]. Later Lee [15] adopted a different thermodynamic model for the Sn-rich solid solution phase (β-Sn). Fries and Lukas [16] also assessed the system but used different unary data and a different temperature dependence of the zinc solubility in pure tin. The eutectic point is observed at 14.8 at.% Zn and 198.25°C. Fries and Lukas results [16] were selected for the COST 531 thermodynamic database [17, 18].

2.4. Ni–Sn–Zn system

The Ni–Sn–Zn system was investigated extensively during the last years [19-29]. Gandova et al. [19] constructed a tentative isothermal section of the Ni–Sn–Zn phase diagram at 873 K. Four more isothermal sections were reported in the literature at different temperatures [20-23]. Liquidus temperatures were obtained using differential scanning calorimetry (DSC). Gandova et al. [24] investigated the system with isopleths at different Ni content. The partial and integral enthalpies of mixing of liquid Ni–Sn–Zn alloys were determined at 1073 K by Plevachuk et al. [25]. The ternary Ni–Sn–Zn system was studied by using diffusion couples technique [26-29].

The three elements (Ni, Sn, Zn) and the respective binary phase diagrams were included in the thermodynamic database developed by the European concerted action [17, 18].

Table 1 presented crystal structure data and their homogeneity ranges in the binary systems.

3. Experiment

Diffusion couples of solid/liquid type were prepared. Each solid part consisted of a solid Ni while the respective liquid part contained preliminary synthesized Sn–Zn alloys with known Sn:Zn ratio (Table 2). Granules of Sn and Zn (p.a.) and 99.99% pure Ni were used for the experiments. Three different compositions (i.e. corresponding to different Sn/Zn ratios) of the Sn–Zn melts were chosen. Evacuated borosilicate glass tubes, containing Sn and Zn (around 10 g) in the desired ratio and a cubic of nickel were prepared. The annealing of the diffusion couples was performed at 400^0 C for 5 days and 450^0 C for 8 days. At the experimental conditions the molten Sn–Zn alloys surrounds the solid Ni thus forming a solid/liquid (Ni)/(Sn+Zn) diffusion couples. After annealing the ampoules were quenched in cold water, and the samples were prepared for a scanning electron microscope characterization. The chemical composition of selected points was measured by an energy-dispersive spectroscopy (EDS) analysis. The concentration of Ni, Sn and Zn was obtained by quantifying the corresponding characteristic X-ray peaks (Mα, Kα and Lα, respectively).

Vickers microhardness of selected phases was measured using a PMT-3 device, applying a diamond pyramid as indenter. This method allows choosing the spot (point) where the measurement has to be done. In this study, a load of 50 g was applied for each measurement. Every phase in a sample was measured between 5 to 10 times, depending on the scattering of the microhardness values.

Table 2 presents the length of the diffusion couples experiment, the different Sn:Zn ratio and and annealing temperature.

Table 2. *Description of diffusion couple experiments of the systems Ni–Sn–Zn. Time of the annealing, days; Ratio – atomic ratio between Sn and Zn content of the liquid phase; t,^{0}C – annealing temperature.*

No	Time, d	Ratio (Sn:Zn)	t, °C
1	5	3:1	400
2	5	1:1	400
3	5	1:3	400
4	8	3:1	450
5	8	1:1	450
6	8	1:3	450

Table 1. *Description of the phases relevant to the Ni–Sn–Zn system*

Phase	Binary system	Composition at. %	Pearson Symbol	Space group	Prototype	Literature
Ni_3Sn_HT	Ni–Sn	24.1 ~ 26.3 at. % Sn	cF16	$Fm\bar{3}m$	BiF3	[31]
Ni_3Sn_LT	Ni–Sn	24.8 ~ 25.5 at. % Sn	hP8	P63/mmc	Mg_3Cd	[31]
Ni_3Sn_2_HT	Ni–Sn	36.7 ~ 44 at. % Sn	hP6	P63/mmc	Ni_2In	[31]
Ni_3Sn_2_LT	Ni–Sn	39.3 ~ 41.1 at. % Sn	oP20	P63/mmc	Ni_3Sn_2	[31]
Ni_3Sn_4	Ni–Sn	53 ~ 57 at. % Sn	mC14	C2/m	Ni_3Sn_4	[31]
β (NiZn)	Ni–Zn	47.5 ~ 58.5 at. % Zn	cP2	$Fm\bar{3}m$	CsCl	[30]
β1(NiZn)	Ni–Zn	45.5 ~ 52 at. % Zn	tP2	P4/mmm	AuCu	[30]
γ(Ni_5Zn_{21})	Ni–Zn	70 ~ 85 at. % Zn	cI52	$I\bar{4}3m$	Cu_5Zn_8	[30]
δ($NiZn_8$)	Ni–Zn	89 at.% Zn	mC28	C2/m	$CoZn_{13}$	[30]

4. Results and Discussion

The experimental results obtained in this work after SEM analyses are shown in Tables 3. In most cases the predominant phases are Ni_3Sn_4, T1 and γ - Ni_5Zn_{21}.

Micrographs of samples N° 1, 3 and 6 from diffusion couple experiments (Table 2) are shown in Figs. 1, 3 and 5, respectively. Layers of Ni_3Sn_4 and the ternary compound T1 have grown at 400 ^{0}C between (Ni) and the former liquid phase with initial Sn:Zn atomic ratio of 3:1 (Fig. 1). All binary phases from the Ni–Zn system and Ni_3Sn_LT and Ni_3Sn_2_LT from the Ni–Sn system were not observed at that composition. Fig. 2 shows the x-ray spectrum of the ternary compound T1. All three elements Ni, Sn, and Zn are observed which confirms the presence of T1 in the sample.

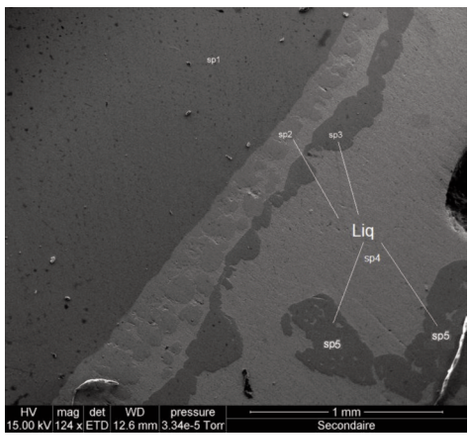

Figure 1. *Micrograph of sample 1 (Table 2) in back scattered electrons. The phases grown at 400^0 C between pure solid nickel and liquid phase with tin/zinc ratio of 3/1 are shown. Sp1 – (Ni), Sp2 – T1, Sp3, Sp5 – Ni_3Sn_4, Sp4 – L – Sn.*

Table 3. *Results of microscope analysis of diffusion couples Ni/Sn–Zn. N° – specimen's number; X_{ij} – constituent's mole fraction obtained in selected spots; phases – identified phases; Remarks – supplementary notes.*

N°	Spectrum No	X_{Ni}	X_{Sn}	X_{Zn}	Phases	Remarks
1	Spectrum 1	0.995	0.005	0.000	Fcc-Ni	Dark phase
	Spectrum 2	0.347	0.412	0.241	T1	The light gray layer
	Spectrum 3	0.431	0.563	0.006	Ni_3Sn_4	Gray layer
	Spectrum 4	0.000	0.979	0.021	L-Sn	The light matrix
2	Spectrum 1	0.996	0.003	0.001	Fcc-Ni	Dark phase
	Spectrum 2	0.431	0.563	0.006	Ni_3Sn_4	Gray layer
	Spectrum 3	0.391	0.447	0.162	T1	The light gray layer
3	Spectrum 1	0.999	0.001	0.000	Fcc-Ni	Dark phase
	Spectrum 2	0.343	0.417	0.240	T1	The light gray layer
	Spectrum 3	0.149	0.040	0.811	γ - Ni_5Zn_{21}	Dark grey layer
	Spectrum 4	0.006	0.912	0.082	L-Sn	The light matrix
	Spectrum 5	0.264	0.011	0.725	γ - Ni_5Zn_{21}	Dark grey layer
	Spectrum 6	0.341	0.412	0.247	T1	The light gray layer
	Spectrum 7	0.161	0.027	0.812	γ - Ni_5Zn_{21}	Dark grey layer
	Spectrum 8	0.154	0.033	0.813	γ - Ni_5Zn_{21}	Dark particles
4	Spectrum 1	0.358	0.441	0.201	T1	The light gray layer
	Spectrum 2	0.420	0.572	0.008	Ni_3Sn_4	Grey phase
	Spectrum 3	0.003	0.959	0.038	L-Sn	The light matrix
	Spectrum 4	0.349	0.415	0.236	T1	The light gray layer
	Spectrum 5	0.080	0.840	0.080	L-Sn	The light matrix
5	Spectrum 1	0.999	0.001	0.000	Fcc-Ni	Dark phase
	Spectrum 2	0.484	0.290	0.226	T1	The light gray layer
	Spectrum 3	0.438	0.561	0.001	Ni_3Sn_4	Grey phase
	Spectrum 4	0.010	0.975	0.015	L-Sn	The light matrix
6	Spectrum 1	0.988	0.003	0.009	Fcc-Ni	Dark phase
	Spectrum 2	0.248	0.013	0.739	γ - Ni_5Zn_{21}	Dark grey layer
	Spectrum 3	0.422	0.172	0.406	T1	The light gray layer
	Spectrum 4	0.072	0.840	0.088	L-Sn	The light matrix

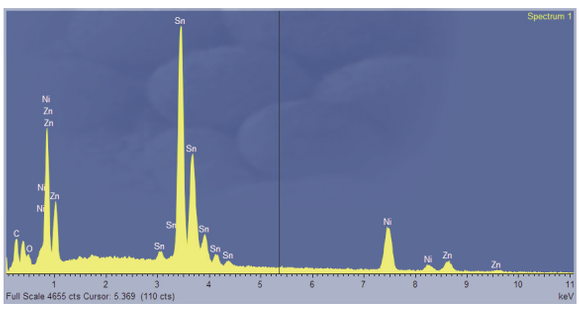

Figure 2. *Picture after SEM analyze of sample 1 with chemical composition of ternary compound T1.*

The micrograph of sample N^{o} 3 (Fig. 3) shows layers of γ-phase (Ni_5Zn_{21}) and the ternary compound T1, which has grown between (Ni) and liquid phase at 400 ^{0}C. In the latter case the initial tin vs. zinc atomic ratio is 1:3. Except for the Ni_5Zn_{21} no other binary intermetallics are observed. Fig. 4 presents the concentration profile of the same sample after the SEM analyze. According to the results, the sample contains no oxygen which confirms that the zinc did not oxidize during the heat treatment.

Fig. 5 (sample 6, Table 2) shows grown layers of ternary compounds T1 and γ-phase (Ni_5Zn_{21}) at 450 ^{0}C between the nickel and the liquid phase with Sn vs. Zn ratio of 1:3. No intermetallics from the Ni-Sn binary system are observed.

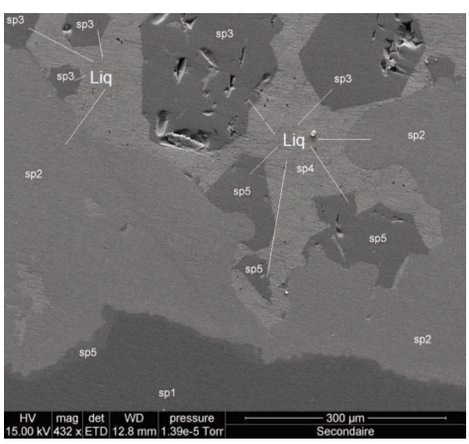

Figure 3. *Micrograph of sample 3 (Table 2) in back scattered electrons. The phases grown at 400 ^{0}C between pure solid nickel and liquid phase with tin/zinc ratio of 1/3 are shown. Sp1 – (Ni), Sp2 – ternary compound T1, Sp3, Sp5 – γ - Ni_5Zn_{21}, Sp4 – L – Sn.*

The results of the microhardness measurements of the Ni–Sn–Zn intermetallic compounds, obtained using a load of 50 g are shown in Table 4. For verification, the nickel and the liq-Sn phase microhardness in all samples was measured. According the results, the hardest phase was γ-Ni_5Zn_{21} followed by T1 except Ni while the softest phase was liquid Sn.

Table 4. *Results of microhardness measurements of the intermetallic layers in the ternary system*

No	Liquid Sn	Fcc-Ni	Ni_3Sn_4	γ-	T1
	H, MPa	H, MPa	H, MPa	H, MPa	H, MPa
1	69	164	556		661
2	38	168			712
3	60	150		815	690
4	55	188	586		642
5	64	190		905	702
6	70	170			706

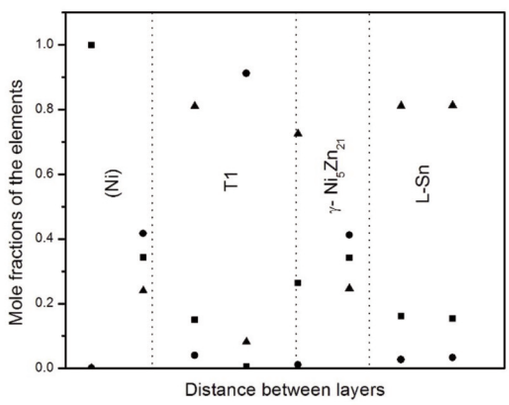

Figure 4. *The composition profile of diffusion layers in sample 3 (the dash lines presented the distance between the layers). Arbitrary distance is plotted along the abscissa, and the measured mole fractions of the elements (X_{Ni}-■, X_{Sn}-●, X_{Zn}-▲)- along the ordinate.*

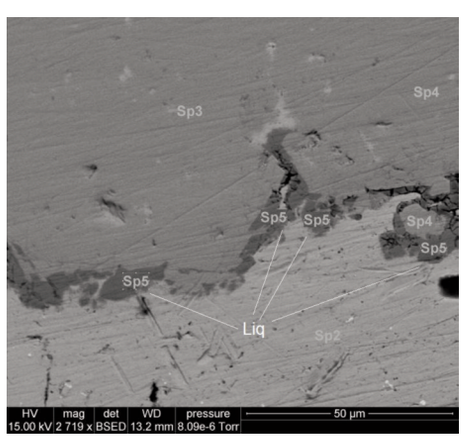

Figure 5. *Micrograph of sample 6 (Table 2) in back scattered electrons. The phases grown at 450 ^{0}C between pure solid nickel and liquid phase with tin/zinc ratio of 3/1 are shown. Sp2 – L – Sn, Sp3, Sp4 – ternary compound T1, Sp5 – γ - Ni_5Zn_{21}.*

The results of this work were used to construct the diffusion paths in the ternary Ni–Sn–Zn system (Fig. 6 and Fig. 7). Fig. 6 presents the diffusion paths for samples 1-3 (Table 2) superimposed with the

calculated phase diagram at the same temperature 400 ^{0}C. All of them start from the liquid phase and converge into pure nickel. One passes along phases connected with Ni–Zn system, another along phases connected with Ni–Sn system but all paths end at the ternary compound T1. Such absences of some equilibrium phases are observed often when diffusion couple experiments are performed and can be explained by nucleation difficulties connected with negligibly thin layer of the pertinent phases.

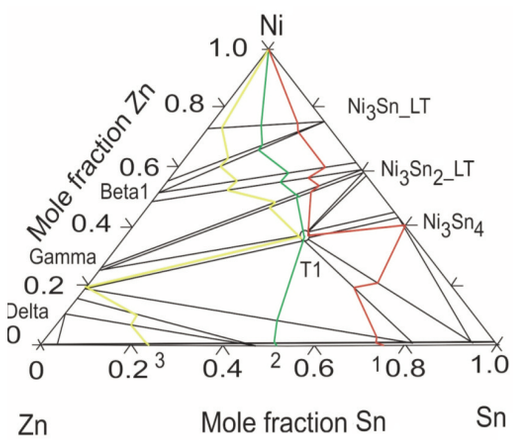

Figure 6. *Diffusion paths in the ternary Ni–Sn–Zn system obtained in this work. 1, 2 and 3 – diffusion paths registered with samples 1, 2 and 3, respectively annealing at 400 ^{0}C.*

The similar results were seen in Fig. 7. Diffusion paths for samples 4-6 (Table 2) are shown on the calculated phase diagram at the same temperature 450 ^{0}C. All paths start from the liquid phase and finish into pure nickel and the ternary compound T1.

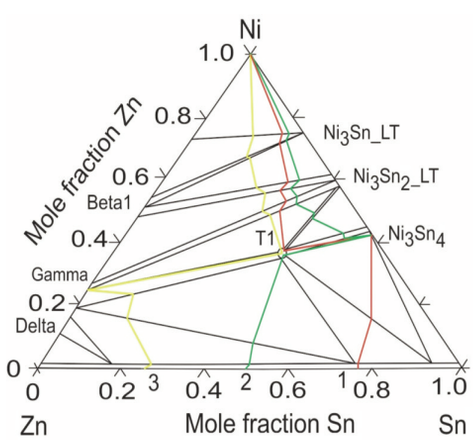

Figure 7. *Diffusion paths in the ternary Ni–Sn–Zn system obtained in this work. 1, 2 and 3 – diffusion paths registered with samples 4, 5 and 6, respectively annealing at 450 ^{0}C.*

Conclusions

Diffusion couples in the Ni–Sn–Zn system were prepared and investigated by scanning electron microscope at two temperatures: 400^0 C and 450^0 C and by microhardness measurements. Experimental data about the diffusion paths was obtained. The existence of the ternary compound T1 in the Ni–Sn–Zn system is confirmed by diffusion couples technique. In the Ni–Sn–Zn system, depending on the initial composition of the liquid phase in th diffusion couple, the diffusion paths go either through the ternary compound T1 or through the γ-Ni_5Zn_{21} phase or Ni_3Sn_4.

Acknowledgements

The author is grateful acknowledge to Professor G. Vassilev for financial support by University of Plovdiv under contract PC09-ХФ-023/09.04.2009.

References

[1] Official Journal of the European Union (L37), 2003, p.19. (http://europa.eu.int/eur-lex/lex/JOHtml.do?uri=OJ:L:2003:037:SOM:EN:HTML)

[2] G. Vassilev, European fundamental Lead-free soldering reserach, Bulg. Chem. And Industry, 78 (2007) 23-32.

[3] A. Mikula, Yazawa International Symposium, Metallurgical and Materials Processing: Principles and Technologies. Volume 1: Materials Processes Fundamentals and New Technologies. Edited by F. Kongoli, K. Itagaki, C. Yamauchi and H.Y. Sohn, TMS The Minerals, Metals & Materials Society, 2003.

[4] G. Ghosh, Metall. Mater. Trans. A., 30 A (1999) 1481-1494.

[5] J. Miettinen, CALPHAD, 27 (2003) 309-318.

[6] H. S. Liu, J. Wang, Z. P. Jin, CALPHAD, 28 (2004) 363-370.

[7] G. P. Vassilev, K. I. Lilova, J. C. Gachon, Therm. Acta, 447 (2006) 106-108.

[8] H. Flanderfer, U. Saeed, C. Luef, A. Sabbar, H. Ipser, Thermochim. Acta, 459 (2007) 34-39.

[9] W. Riesenkampf, T. Biestek, J. Morgiel, W. Lasocha, , J. of Mater. Sci., 36 (2001) 4633-4636.

[10] P. Glibin, T.N. Vorobyova, B. V. Kuznetsov, Thermochim. Acta, 507-508 (2010) 35-40.

[11] G. P. Vassilev, T. Gomez-Acebo, J-C. Tedenac, J. Phase. Equilib., 21 (2000) 287-301.

[12] G. P. Vassilev, J. Phase Equil. and Diffusion, 26 (2005) 309–310.

[13] W. Xiong, H. Xu, Y. Du, Calphad, 35(3) (2011) 276-283.

[14] M. Srivastava, R. C. Sharma, J. Phase. Equilb., 14 (1993) 700-709.

[15] B-J. Lee, CALPHAD, 20 (1996) 471-480.

[16] S. Fries, H. Lukas, Unpublished work, 2002.

[17] A. Dinsdale, A. Watson, A. Kroupa, J. Vrestal, A. Zemanova, J. Vizdal, Atlas of Phase Diagrams for the Lead-Free Soldering, COST 531 (Lead-free Soders), Vol. 1, © COST office, 2008.

[18] A. Kroupa, A. Dinsdale, A. Watson, J. Vrestal, A. Zemanova, P. Broz, J. Min. Metall. Sect. B-Metall., 48 (3) B (2012) 339-346.

[19] V. Gandova, D. Soares, K. Lilova, J. C. Tedenac, G. P. Vassilev, Phase equilibria in the system Sn–Zn–Ni , Int. J. Mater. Res., 3 (2011) 257-268.

[20] J. Chang, S. K. Seo, H. M. Lee, J Electron Mater., 39 (2010) 2643-2652.

[21] J. L. Liang, Y. Du, Y. Y. Tang, J. Electron Mater. 40 (2011) 2290-2999.

[22] S. Chen, C. Hsu, C. Chou, C. Hsu, Progress in Natural Science: Materials International., 21(2011) 386-391.

[23] C. Schmetterer, D. Rajamohan, H. Ipser, H. Flandorfer, Intermatalics., 19 (2011) 1489-1501.

[24] V. D. Gandova, P. Brozb, J. Bur˘sík , G. P. Vassilev, Thermochimica Acta., 524 (2011) 47-55.

[25] Yu. Plevachuk, A Yakymovych, S. Fu¨rtauer, H. Ipser, H. Flandorfer, Journal of Phase Equilibria and Diffusion, 35 (4) 359-368.

[26] W. Zhu , H. Liu, J. Wang, J. Electron. Mater, 39 (2010) 209-214.

[27] C. Wang, H. Chen, J. Electron. Mater.,39 (2010) 2375-2381.

[28] C. Wang, H. Chen, W. Lai, J. Electron. Mater., 40 (2011) 2436-2444.

[29] Y. Yuan, D. Li, L. Liu, G. Borzone, J. Electron. Mater., 41 (2012) 2495-2501.

[30] T. Massalski, CD ROM: Binary Alloy Phase Diagrams, ASM International, OH, USA, 1996.

[31] C. Schmetterer, H. Flandorfe, K. W. Richter, U. Saeed,. M. Kauffman, P. Roussel, H. Ipser, Intermetallics. 15 (2007) 869-884.